

Cite this: DOI: 10.1039/c2lc20586f

www.rsc.org/loc

PAPER

Biochemical sensor tubing for point-of-care monitoring of intravenous drugs and metabolites†

Charles J. Choi,[‡] Hsin-Yu Wu,^a Sherine George,^b Jonathan Weyhenmeyer^a and Brian T. Cunningham^{*ab}

Received 30th June 2011, Accepted 30th November 2011

DOI: 10.1039/c2lc20586f

In medical facilities, there is strong motivation to develop detection systems that can provide continuous analysis of fluids in medical tubing used to either deliver or remove fluids from a patient's body. Possible applications include systems that increase the safety of intravenous (IV) drug injection and point-of-care health monitoring. In this work, we incorporated a surface-enhanced Raman scattering (SERS) sensor comprised of an array of closely spaced metal nanodomains into flexible tubing commonly used for IV drug delivery and urinary catheters. The nanodome sensor was fabricated by a low-cost, large-area process that enables single use disposable operation. As exemplary demonstrations, the sensor was used to kinetically detect promethazine (pain medication) and urea (urinary metabolite) within their clinically relevant concentration ranges. Distinct SERS peaks for each analyte were used to demonstrate separate detection and co-detection of the analytes.

Introduction

In the clinical environment, the most widely used method for administering liquid-based materials to a patient is through intravenous (IV) delivery. Infusion pumps or gravity-driven flow through flexible plastic tubing are used to deliver fluids, nutrients, and drugs to patients. Likewise, plastic tubing is the predominant liquid-handling method used for urinary catheterization and all types of dialysis.

For detection and identification of analytes in a clinical setting, it is not generally permissible to introduce materials such as chemicals, enzymes, or nanoparticle tags into the liquid media for the sole purpose of facilitating detection. This is true particularly for detection of biochemicals within liquids that are being delivered into a person. For this reason, there is a strong preference to utilize “label-free” detection methods, provided that sufficient sensitivity and selectivity are available. There is also a strong motivation to develop detection methods that can provide continuous information at the point of care, in order to avoid periodic sampling of fluid from tubing connected to patients, which adds a risk of introducing infection and requires tests to be carried out in a separate diagnostic laboratory.

Therefore, it is our goal to incorporate label-free sensors into the internal surfaces of plastic tubing to enable continuous in-line monitoring of the chemical components of the material flowing through the tubing.

In this work, detection of IV pain medication (promethazine) and a common urinary metabolite (urea) were used as models to demonstrate the potential for continuous monitoring of an IV delivered drug or kidney function of a patient. A recently developed surface-enhanced Raman scattering (SERS) nanodome structure that is produced upon flexible plastic surfaces by a large-area nanoreplica molding process is used as the sensor. The nanodome structure provides enhancement of the electromagnetic field from a laser illumination source to provide an easily measurable SERS spectrum that specifically identifies the analyte of interest. We demonstrate both separate detection and co-detection of promethazine and urea within their clinically relevant concentration ranges, as well as kinetic real-time monitoring of changes in analyte concentration.

Background

Drug compound – promethazine. Medication errors occurring either in or out of the hospital are estimated to account for 7000 deaths annually, while infusion devices account for up to 35% of errors that result in significant harm (Class 4 and 5).¹ Current “smart” IV medication safety systems reduce medication delivery errors by providing standard modular-based guidance of the dose and infusion rate through various types of IV administration to the clinicians without the use of sensors.² Identification and verification of the chemical contents of a fluid in an IV line being administered to a patient would provide an additional

^aDepartment of Electrical and Computer Engineering, Micro and Nanotechnology Laboratory, University of Illinois at Urbana-Champaign, 208 North Wright Street, Urbana, IL, 61801, USA. E-mail: bcunning@illinois.edu

^bDepartment of Bioengineering, Micro and Nanotechnology Laboratory, University of Illinois at Urbana-Champaign, 208 North Wright Street, Urbana, IL, 61801, USA

† Electronic supplementary information (ESI) available. See DOI: 10.1039/c2lc20586f

‡ The author is now at the National Institute of Standards and Technology (NIST), 100 Bureau Drive, Gaithersburg, MD 20899, USA.

layer of error-checking to ensure that the correct drug and dosage are being delivered.

Promethazine is part of the phenothiazine chemical class that is used medically as an antihistamine, a sedative, and an antiemetic. The maximum recommended concentration for IV administration of promethazine is 25 mg mL^{-1} , and overdose can cause severe tissue injury including gangrene, requiring fasciotomy, skin graft, and/or amputation.³

Metabolite – urea. Annually, more than 300 million urine analyses are ordered by physicians in the United States.⁴ Urine tests are very useful as noninvasive diagnosis and evaluation of kidney function and health of a patient. Urea is the main and final product of protein metabolism; thus its concentration in urine is used as an indicator of the nutritional status of a patient, while its concentration in blood is useful for diagnosis of renal dysfunction. During kidney dialysis, urea is recognized as a marker for a wide spectrum of low and intermediate-molecular mass toxic solutes that accumulate in patients with diminished renal function.⁵ Normal physiological levels of urea concentration in blood and urine are 2.5–6.7 mM and $\sim 333 \text{ mM}$, respectively. In comparison to this normal level, the pathophysiological concentration of urea in blood is 30–150 mM, which indicates lost kidney function due to renal clearance failure.^{4,6} In the case of kidney failure, renal replacement therapy in the form of dialysis and transplantation is required in order to sustain the life of a patient.

The most common method for urea detection is an enzyme-based colorimetric approach using spectrophotometric detection.⁷ However, the colorimetric method involves introduction of additional chemicals/enzymes to fluid samples that could potentially harm patients, and thus is performed by taking a urine sample to a laboratory for analysis. In addition, reagent mixing and incubation steps required for the colorimetric detection make the method unsuitable for real-time monitoring of bodily fluid.

A number of label-free urea sensing methods have been developed including enzyme-based field effect transistors (ENFETs), ion sensitive field effect transistors (ISFETs), conductometric, potentiometric and optical fiber sensors.^{6,8–13} These sensors involve immobilization of a capture probe molecule, urease enzyme, on the surface of the gate insulator or the sensor. However, uncertainties and variations are associated with label-free sensors immobilized with enzymes. These variations are caused by interference from ammonia and other ionic substances or by change in solution temperature and pH, decreasing the enzyme activity and stability.⁶ In addition, immobilization methods involving cross-linking cause loss of protein flexibility and hinder the diffusion of analytes, resulting in sensor performance (sensitivity, response time) that is dependent on the method of enzyme immobilization.⁹ Therefore, a label-free sensor without the requirement for enzyme or probe molecule immobilization is desirable.

Infrared (IR) absorption spectroscopy has also been used to detect urea in urine by transmitting a selected band of near-IR light through the sample and analyzing the resulting spectral information.¹⁴ The IR absorption spectroscopy method does not involve probe molecule immobilization and is nondestructive and reagentless, thereby permitting in-line identification.

However, due to the relatively high detection limit and heterogeneous characteristic of bodily fluid, blood in particular, it is difficult to detect urea with sufficient accuracy.

Raman spectroscopy and surface-enhanced Raman scattering (SERS)

Raman spectroscopy is a powerful and versatile tool for label-free molecular detection and identification. By measuring the vibrational energies associated with chemical bonds, Raman spectroscopy is able to identify unique chemical signatures in complex mixtures. As first observed and theoretically understood, the extremely small Raman scattering cross section may be enhanced when a molecule is in close proximity to a roughened metal surface that supports regions of heightened electromagnetic field intensity.^{15,16} This enhancement is known as surface-enhanced Raman scattering (SERS). The enhancement of the local electromagnetic field at the surface of a metal with respect to the incident field for SERS originates from localized surface plasmon resonance (LSPR).¹⁷ This electromagnetic enhancement effect results in enhanced excitation of Raman vibrational modes. Therefore, SERS enables Raman scattering spectra to be gathered effectively and with substantially less laser power, enabling many new detection applications, provided that the analytes have an opportunity to come into contact with the SERS-active surface.

In this work, we focus upon incorporation of a SERS active surface comprised of an array of closely spaced metal nanodomains into a plastic flow chamber connected in series with flexible tubing as shown in Fig. 1. Fig. 1b shows a scanning electron microscope (SEM) image of the nanodome sensor structure incorporated as the bottom surface of the flow cell. Fig. 1c shows a finite element method (FEM) simulation of the electric field distribution around the nanodomains, in which the greatest electromagnetic fields occur in the gaps between adjacent nanodomains. For SERS surfaces to be viable for an application in which they would be used as a single-use disposable point-of-care sensor, it is necessary to provide a structure that simultaneously

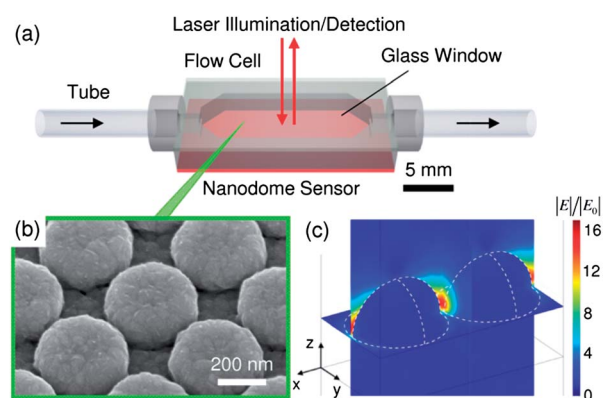


Fig. 1 (a): Schematic of the biochemical sensor tubing where nanodome sensor structure is incorporated as the bottom surface of the flow cell. (b): SEM image of the nanodome surface. (c): 3D FEM simulation of the electric field distribution (normalized amplitude of the electric field with respect to the incident electric field amplitude) displaying regions of enhanced field between adjacent nanodomains.

provides a large electromagnetic enhancement factor (EF) and is made using a low-cost, large-area manufacturable fabrication method. The SERS nanodome sensor used in the present study provides label-free identification/detection of analytes without having to immobilize probe molecules on the sensor surface. The nanodome surface used in the present study is produced on a flexible plastic substrate by a large-area nanoreplica molding process to provide peak EF of 1.37×10^8 .¹⁸ The exemplary experiments on the detection of promethazine and urea demonstrate the clinical potential for SERS sensors incorporated within biomedical tubing. The system could enhance patient safety through prevention of drug delivery errors that occur by administering an incorrect drug or dose, and provide more timely information on the status of a patient through monitoring of urinary metabolite concentration.

Materials and methods

Nanodome sensor fabrication – nanoreplica molding process

The cross section diagram of the nanoreplica molding process is shown in Fig. 2. To produce a template used for the molding, nanoimprint lithography (Molecular Imprints) and reactive ion etching were used to pattern an 8-inch (200 mm) diameter silicon wafer with a 2-dimensional array of 300 nm diameter holes (period = 400 nm, depth = 130 nm), in $8 \times 8 \text{ mm}^2$ dies with overall feature dimensions of $120 \times 120 \text{ mm}^2$. Next, a negative volume image of the silicon surface structure was formed by

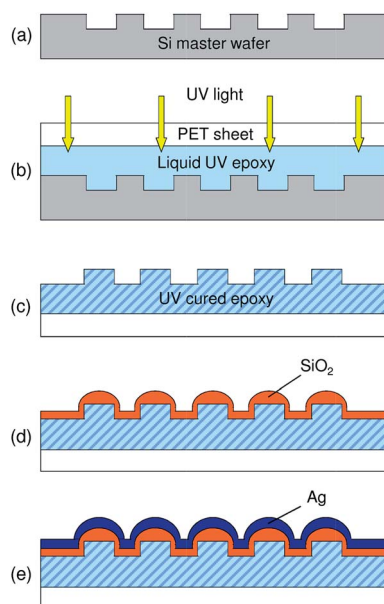


Fig. 2 Cross section diagram of the nanoreplica molding process. (a): Fabrication of silicon master wafer template with 400 nm period 2D circular hole structure using nanoimprint lithography and reactive ion etching to a depth of 130 nm. (b): Distribution of liquid-state UV curable polymer between the silicon master wafer and the PET substrate with subsequent solidification by UV light exposure. (c): Release of the PET substrate, resulting in a polymer replica of the silicon wafer structure adhered to the PET sheet. (d)-(e): Deposition of SiO_2 followed by Ag on the replicated surface using electron-beam evaporation. Used with permission from the IOP Publishing.

dispensing liquid UV curable polymer (Gelest) droplets (total volume of $\sim 200 \mu\text{L}$) and distributing between the silicon wafer and a $250 \mu\text{m}$ thick flexible polyethylene terephthalate (PET) sheet using a roller. Based on the polymer dispense volume and the distributed area, the spacing between the silicon wafer and the PET sheet is $\sim 10 \mu\text{m}$. After curing by exposure to UV light, the molded structure was released from the wafer by peeling away the PET, resulting in a polymer replica of the silicon wafer structure adhering to the PET sheet. Then, 100 nm of SiO_2 was deposited over the polymer replica by electron beam evaporation, followed by deposition of a 200 nm silver thin film, also by electron beam evaporation, to complete the device. The cylindrical posts created by the replica molding process evolved into rounded dome-like shapes as the deposited films accumulated. The separation distance for the nanodome array was 20 nm with the nanodome base diameter of 380 nm. The details of nanodome fabrication using nanoreplica molding process are described in a previous publication.¹⁸

Flow cell incorporated with nanodome sensor

The flow cell was made with a stereolithography system (Viper SLA system, 3D Systems) using an optically clear resin (Water-Clear Ultra 10122, DSM Somos). The dimensions of the flow chamber were $18.5 \times 7.5 \times 3 \text{ mm}$ for length, width, and height, respectively. Inlet/outlet cross sectional dimensions of the flow cell were $3 \times 1 \text{ mm}$. Two cylindrical openings at the ends of the flow cell were tapped and screwed in with polypropylene barbed adapters ($10\text{--}32 \text{ UNF} \times 1/8'' \text{ ID}$, Cole-Parmer) connected to tubing ($1/8'' \text{ ID} \times 3/16'' \text{ OD}$, TYGON R-3603). The nanodome surface was cut and attached as the bottom surface of the flow cell using UV-cured adhesive (Addison Clear Wave). The top surface window of the flow cell was sealed by attaching a standard No. 2 microscope slide cover glass cut to size using the same UV adhesive.

Detection instrument

A schematic of the detection instrument for Raman measurement on nanodome sensor tubing is shown in Fig. 3. The Raman measurement was performed using a 785 nm wavelength diode laser system (Ocean Optics) coupled into an optical fiber. For detection of promethazine, the laser power was set to 100 mW. For detection of urea and urea/promethazine mixture, the laser was set to 150 mW. The laser was focused on the sensor surface

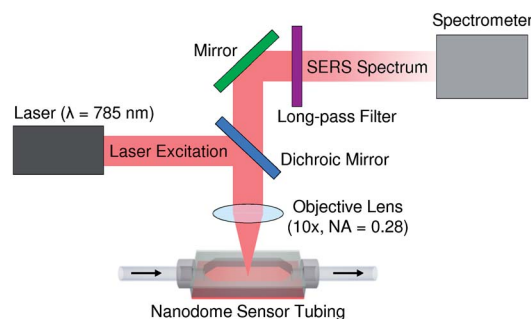


Fig. 3 Schematic of the detection instrument used for Raman measurement on nanodome sensor tubing.

by a 10x objective lens (NA = 0.28). SERS photons were collected by the same objective lens, into a spectrometer (QE65000, Ocean Optics) using an integration time of 5 s for all experiments.

Experiment procedures

Experimental procedures were identical for promethazine and urea as well as for the promethazine/urea mixture. For the concentrations series measurements, promethazine solution was prepared in DI water at 50, 25, 12.5, 6.25, 3.13, and 1.56 mg mL⁻¹. Urea solution was prepared in concentrations of 300, 100, 75, 50, and 25 mM in artificial urine. The artificial urine solution was prepared according to a previously published formula.^{19,20} The artificial urine solution was made by mixing 1.1 mM lactic acid, 2.0 mM citric acid, 25 mM sodium bicarbonate, 2.5 mM calcium chloride, 90 mM sodium chloride, 2.0 mM magnesium sulfate, 10 mM sodium sulfate, 7.0 mM potassium dihydrogen phosphate, 7.0 mM dipotassium hydrogen phosphate, and 25 mM ammonium chloride in DI water (all reagents were purchased from Sigma-Aldrich). Urea and promethazine mixture was prepared in three combinations of concentrations in DI water: 300 mM, 25 mg mL⁻¹; 150 mM, 25 mg mL⁻¹; 300 mM, 12.5 mg mL⁻¹ for urea and promethazine, respectively. Before the SERS measurement, 5 mL of analyte solution was pumped through the sensor tubing manually using a syringe and measurements were taken without flow. After the measurement, the flow cell was washed by emptying the analyte solution and flowing through 5 mL of DI water. Emptying and rinsing with DI water was repeated three times before introducing another analyte with a different concentration. For statistical significance and to quantify reproducibility of the nanodome sensor tubing, measurements on the analyte concentration series were repeated five times (one measurement per analyte concentration in a series).

For the kinetic on/off measurements, the analyte sample and DI water were alternately pumped through the sensor tubing using a separate syringe pump (PHD 22/2000, Harvard Apparatus) for each solution at 60 s intervals. Tubing from the syringes containing the sample and blank solution were connected to a three-way stopcock valve which was used to alternate the samples flowing into the sensor tubing. The solutions were pumped through the tubing at a flow rate of 5 mL min⁻¹. Although typical IV injection rates are significantly lower, a flow rate of 5 mL min⁻¹ was chosen to facilitate the kinetic experiment and to minimize cross diffusion of analytes at the interface between different solutions as they are being pumped.

For comparison, urea detection was performed using a colorimetric urea assay kit (DIUR-500, BioAssay Systems) with the same urea samples used for the experiment on nanodome sensor tubing. 5 μ L of urea sample for each concentration, standard urea solution (50 mg/dL) and DI water (blank) were transferred into wells of a clear bottom 96-well plate in triplicates. Then, 200 μ L of assay reagent mixture included in the kit was added to each well and incubated for 20 min at room temperature. After incubation, a microplate reader (Synergy HT, BioTek Instruments) was used to measure the optical density of the samples at wavelength of 520 nm.

The nanodome structure reported in this work does not contain any high aspect ratio structures or nanoparticles that are

loosely tethered to the substrate, but rather two thin film coatings that are firmly anchored over the entire surface structure. Due to this robust structure, no metal particle break-off or delamination was observed during or after the experiments for any of the sensors fabricated and tested. To confirm that no surface damage occurs from continuous exposure to aqueous reagents, a long-term SERS measurement (up to 5 days) was performed on the same locations of a nanodome sensor device filled with 1 μ M rhodamine 6G (R6G) solution. The measurement results are shown in Fig. S1 in the Electronic Supplementary Information (ESI). The SEM images of the nanodome surface before and after continuous exposure to deionized water for 5 days are also shown in the ESI (Fig. S2).

Data analysis

The background of the raw SERS spectra was removed using a 6th order polynomial fit, followed by signal filtering using Savitsky-Golay parameters with smooth window of 9 and polynomial order of 3. The processed spectra were then subtracted by the reference spectrum from a blank solution to obtain the final spectra.

Results

Detection of promethazine

Fig. 4(a) compares the SERS spectra for promethazine solutions of varying concentrations from 3.13 to 50 mg mL⁻¹, the range typically delivered to patients. The SERS spectra of promethazine solution exhibited dominant Raman intensity peaks located at 1030 cm⁻¹, due to the ring-breathing mode of the aromatic rings, and at 1567 cm⁻¹ and 1589 cm⁻¹, corresponding to aromatic C=C stretching modes of the molecule.²¹ Using the dominant peak located at 1030 cm⁻¹ for analysis of promethazine, the inset shows the plot of the average Raman intensity as a function of promethazine concentration with error bars indicating ± 1 standard deviation measured from five separate concentration series (N = 5). In each series, a single SERS measurement was made for each analyte concentration, where a wash step consisting of emptying and flowing through 5 mL of buffer solution was repeated three times between each analyte concentration. A linear fit between the Raman intensity at 1030 cm⁻¹ and the concentration of promethazine yielded an R² value of 0.999. This demonstrates that the nanodome sensor tubing may be used to identify promethazine in solution and the Raman peak magnitude is linearly proportional to its concentration.

In order to investigate the real-time detection capability of the nanodome sensor, SERS measurements were made with 50 mg mL⁻¹ promethazine solution and DI water alternately pumped through the tubing at 60 s intervals. Measurements were taken every 5 s, the same as the integration time of the spectrometer. Fig. 4(b) shows the kinetic plot of Raman intensity measured at 1030 cm⁻¹ as a function of time. The results indicate that real-time monitoring of solution flowing through tubing can be achieved for the nanodome sensors. Delay in sensor response can be observed due to analyte molecules diffusing across a stagnant flow layer that forms near the surface of the nanodome sensor as solutions are pumped through the flow cell. Considering the

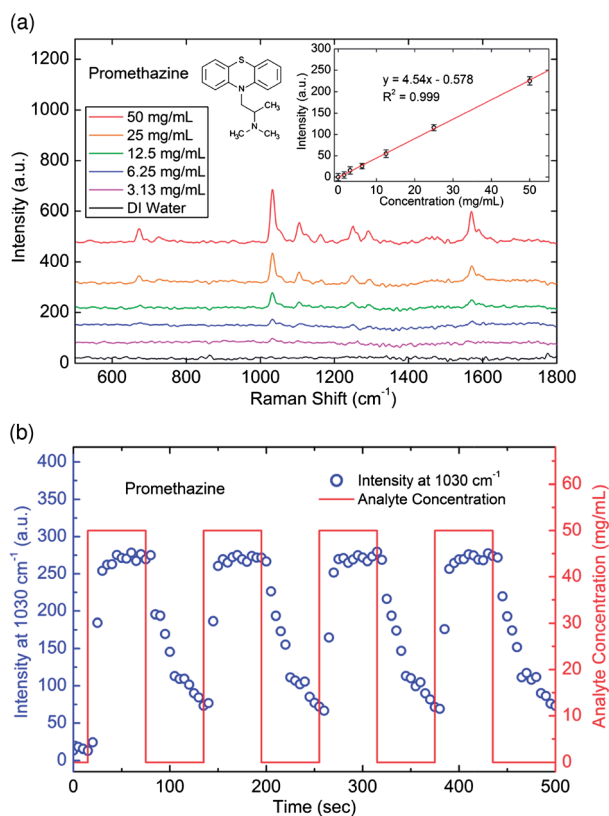


Fig. 4 (a): SERS spectra for promethazine solution within the sensor tubing. Primary Raman intensity peak for promethazine compound corresponding to the ring-breathing mode of the aromatic rings can be observed at 1030 cm^{-1} . Inset: Raman intensity measured at 1030 cm^{-1} as a function of promethazine concentration with error bars indicating ± 1 standard deviation ($N = 5$). (b): Kinetic plot of Raman intensity measured at 1030 cm^{-1} as 50 mg mL^{-1} promethazine solution and DI water were alternately pumped through the tubing at 60 s intervals.

typical injection rate used to administer drugs ($0.0667\text{--}0.1\text{ mL min}^{-1}$ for 25 mg mL^{-1} promethazine injection),³ the delay in sensor response due to diffusion in the stagnant fluid layer should not cause hindrance in detecting medication error before any serious health hazard is posed.

From the kinetic plot, the standard deviation (σ) of the Raman signal measured at 1030 cm^{-1} was 3.51. Based on the linear dose response curve (inset of Fig. 4(a)) and by setting the sensor readout resolution as three standard deviations (3σ), the limit of detection for nanodome sensors on promethazine was 2.32 mg mL^{-1} . The results suggest that the nanodome sensor tubing system is capable of identifying promethazine compounds and detecting concentrations that are clinically relevant. For example, the system could be used to detect and prevent hazards associated with IV-delivered promethazine over the maximum allowed concentration of 25 mg mL^{-1} .

While the promethazine detection data shown here was obtained with the drug diluted in DI water, in the clinic it may also be administered in 0.9% NaCl solution or phosphate buffered saline. We have verified that these buffers do not contribute a background SERS signal that interferes with the detection of promethazine.

Detection of urea

As with promethazine solution, measurements were made for the detection of urea in artificial urine solution flowing through the system. Fig. 5(a) compares the SERS spectra for urea solutions of varying concentrations ranging from 25 to 300 mM, encompassing the range of urea concentration typically measured clinically. Urea in artificial urine solution exhibited a primary Raman intensity peak at 1000 cm^{-1} from the symmetrical C–N stretch.⁴ The inset shows the plot of the average Raman intensity measured at 1000 cm^{-1} as a function of urea concentration with error bars indicating ± 1 standard deviation measured from five separate concentration series ($N = 5$). As in the case for promethazine, in each series a single SERS measurement was made for each analyte concentration where a wash step consisting of emptying and flowing through 5 mL of buffer solution was repeated three times between each analyte concentration. A linear fit with an R^2 value of 0.999 was obtained. Again, this demonstrates that the nanodome sensor tubing may be used to identify urea compound in urine and detect its concentration.

To investigate the real-time detection capability for urea, SERS measurement was made with 300 mM urea solution and blank artificial urine solution alternately pumped through the tubing at 60 s intervals. The same integration time and

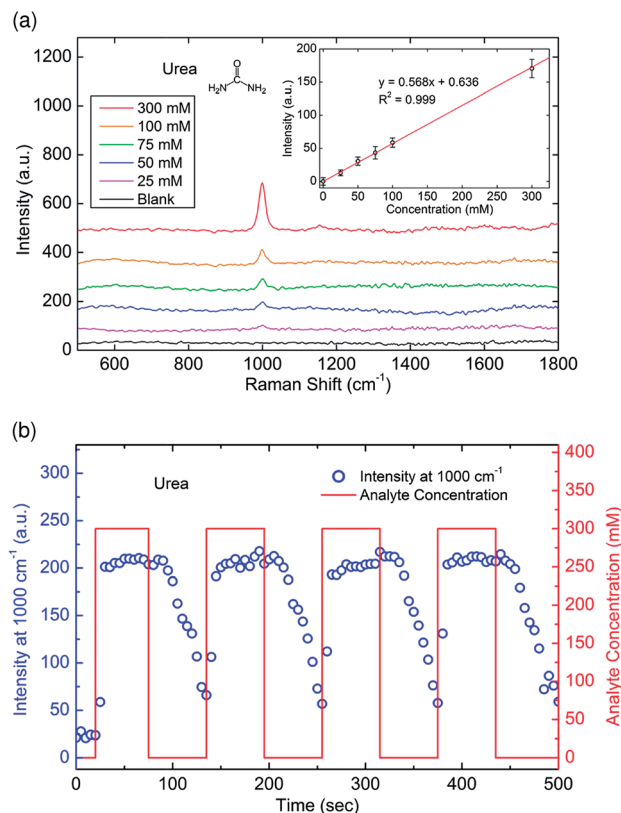


Fig. 5 (a): SERS spectra for urea solution within the sensor tubing. Primary Raman intensity peak for urea corresponding to the symmetrical C–N stretch can be observed at 1000 cm^{-1} . Inset: Raman intensity measured at 1000 cm^{-1} as a function of urea concentration with error bars indicating ± 1 standard deviation ($N = 5$). (b): Kinetic plot of Raman intensity measured at 1000 cm^{-1} as 300 mM urea solution and DI water were alternately pumped through the tubing at 60 s intervals.

measurement interval as with the promethazine experiment were used. Fig. 5(b) shows the kinetic plot of Raman intensity measured at 1000 cm^{-1} as a function of time. Delay in sensor response was observed for the urea measurement as well, but it should not cause issues for real-time detection.

For urea, the standard deviation (σ) for the Raman intensity at 1000 cm^{-1} was 2.68. Based on the linear dose response curve (inset of Fig. 5(a)) and three standard deviation (3σ) threshold for the sensor readout resolution, the limit of detection for urea was 13.0 mM. The results suggest that the nanodome sensor tubing system is capable of monitoring kidney activity of a patient through identifying and detecting urea well below the typical concentration in urine. The system could also be used to monitor renal clearance failure by detecting urea concentration in blood or dialysate since the detection limit of the system is below the pathophysiological concentration of 30–150 mM. In an attempt to focus on detection of urinary metabolites, making SERS measurements in blood was not performed due to additional process steps that may be required such as separating serum from blood cells. However, the potential for performing SERS measurements in blood has been demonstrated, so it may be possible in the future to incorporate sensors into tubing used to withdraw blood from donors or patients.^{22–24}

To verify the accuracy of the nanodome sensor for detection of urea, the same urea samples of various concentrations in artificial urine (9–170 mM) were used for making measurements with both the nanodome sensor and the standard commercially available colorimetric urea assay kit. Fig. 6 shows the sensor output comparison between the nanodome sensor and the standard colorimetric assay kit. For each concentration of urea sample, the output from the nanodome sensor tubing is plotted on the y-axis and the output from the colorimetric assay is plotted on the x-axis. The comparison data was fitted to a $y = x$ curve with an R^2 value of 0.991.

Detection of urea/promethazine mixture

The ability for multiplexed detection of analytes is useful as multiple drugs or nutrients are often delivered to patients

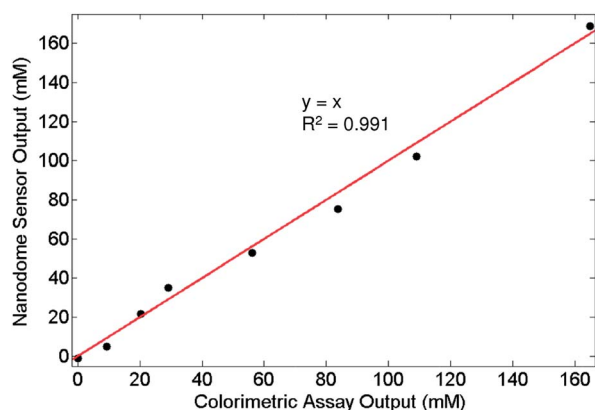


Fig. 6 Sensor output comparison for urea concentration detection between nanodome sensor and standard colorimetric assay kit. For each concentration of urea, the output from the nanodome sensor tubing is plotted on the y-axis and the output from the colorimetric assay is plotted on the x-axis.

through IV lines in clinical settings. One advantage of SERS-based sensors is their capability for detection of multiple analytes simultaneously when the Raman scattered peaks can be individually distinguished. To demonstrate the multiplexed detection capability of the SERS nanodome sensor, mixture solutions of urea and promethazine (in DI water) at varying concentrations were introduced into the sensor tubing. Fig. 7 shows the SERS spectra for the urea and promethazine mixtures where primary Raman intensity peaks for both urea and promethazine can be observed at 1000 cm^{-1} and 1030 cm^{-1} , respectively. The intensity values for each analyte were consistent with measurements made with single analyte solution.

Discussion

An important aspect of this work is the ability to create a surface that supports a SERS enhancement factor (EF) that is substantial enough to enable detection of drugs and metabolites at physiologically relevant concentrations, while using a fabrication process that is amenable to single-use disposable scenarios such as point-of-care diagnostic tests. As shown in previous work, the nanodome surface displays a peak SERS EF of 1.37×10^8 , which compares favorably with structures produced by the deposition of metal films over nanospheres ($\text{EF} = 10^7$) or films comprised of silver nanoparticles dispersed over a surface ($\text{EF} = 10^8$).^{17,25,26} The nanodome structure has demonstrated the ability to perform trace detection of phthalic acid contaminants that are leached from polypropylene containers²⁷ and has thus demonstrated the ability to perform detection of low-concentration analytes in addition to the relatively high concentration analytes demonstrated here. While other structures have demonstrated greater EF through the use of nanofabricated gaps that are defined by electron beam lithography or focused ion beam milling,^{28–30} these structures would not be economically feasible for our intended use, and would not provide additional benefit in terms of detection of the analytes of greatest interest in biomedical tubing.

The reproducibility of chemical analysis from the nanodome sensor tubing was found to be excellent, although several experimental variables are capable of altering the magnitude of the SERS signal. The EF of the nanodome sensor itself is the

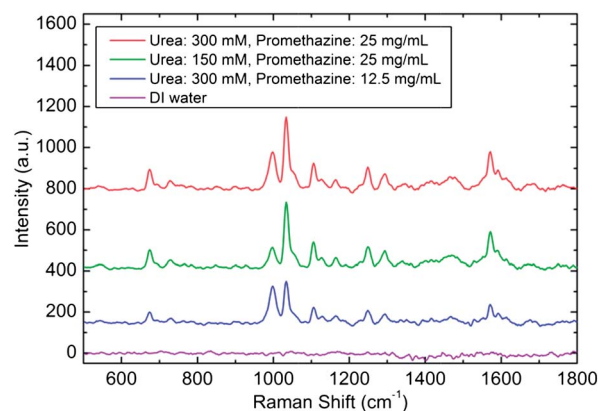


Fig. 7 SERS spectra for urea and promethazine mixture in DI water. Primary Raman intensity peaks for both urea and promethazine can be observed at 1000 cm^{-1} and 1030 cm^{-1} , respectively.

major factor contributing to the magnitude of the SERS output. It is important, therefore, to control the dome-to-dome gap spacing accurately by controlling the thickness of the SiO₂ thin film thickness as described in our previous work.¹⁸ Through the use of an accurately calibrated quartz crystal microbalance during nanodome fabrication, SERS nanodome sensors with consistent interdome spacing, and therefore EF, can be fabricated using our approach – even in a research laboratory environment. In order to illustrate the reproducibility of the nanodome sensor tubing between different sensors, a concentration series experiment using promethazine and urea was repeated using a fresh device from a separate fabrication batch. The comparisons of the results are shown in Fig. S3 in the Electronic Supplementary Information (ESI). The second most important factor impacting SERS signal is the intensity of the laser illumination on the sensor surface. With the illumination/collection objective used in our instrument, the alignment conditions were intentionally lenient. For a system that would be used at the bedside, alignment issues would be addressed by incorporating illumination/collection optics in a small housing unit where the sensor tubing could be reproducibly aligned and clamped using a mechanical fixture that does not require user adjustment. Signal fluctuation due to temperature change was not observed during the experiment.

The number of drug compounds or metabolites that can be detected using this technique is mainly determined by the EF of the SERS substrate and the molecule's ability to produce Raman peak intensities above detectable range. The intensity of the Raman scattered radiation from an analyte molecule depends on the vibrational Raman cross section, which is determined by the change in the molecule's polarizability induced by its vibrational modes.³¹ There has been work done by others in measuring Raman spectra of common pharmaceutical excipients and biological molecules including primary metabolites^{32,33} so extension of the approach shown in this paper to other analytes is feasible.

For the kinetic measurements, the temporal resolution was limited by the integration time used for the spectrometer (5 s). Therefore, lowering the detector integration time would improve the temporal resolution of the kinetic measurements. However, lowering the integration time eventually leads to a decrease in the signal-to-noise ratio (SNR) for the SERS spectra in which case, higher laser illumination power and/or a higher numerical aperture illumination/collection lens could be used to keep the SNR above an acceptable value.

It should be noted that a sensor incorporated in-line with IV drug infusion tubing would be one element of a control system that could be used to rapidly respond to a sensed drug or concentration that is outside prescribed parameters. When an IV medication error event occurs (whether an incorrect drug is being administered or a maximum concentration for a particular drug is exceeded), infusion could be stopped before the drug reaches the patient, for example through the closure of a computer-controlled valve or stoppage of an infusion pump that is in communication with the sensor. Considering the case for promethazine where the infusion rate for a maximum concentration solution (25 mg mL⁻¹) ranges from 0.0667 to 0.1 mL min⁻¹,³ stopping infusion before a lethal dose of chemical reaches the patient would be feasible. Another common lethal scenario is when a whole bag of an incorrect drug or a drug exceeding

maximum concentration is left to be delivered to a patient for a prolonged period of time. With sensors placed in the tubing however, even if the drug reaches the patient due to the delay in the sensor response, the infusion rates are slow enough that the infusion could be stopped before significant harm is done to the patient.

Conclusions

In this paper, we used a SERS nanodome sensor chip incorporated in a flow cell for real-time biochemical sensing of fluid within tubing, and performed proof-of-concept experiments on the label-free detection of urea and promethazine. We have demonstrated the potential for an in-line nanodome sensor detection system that would allow real-time detection of fluid samples from patients without taking samples and performing laboratory based tests. The technology may be applied to identify drug compounds that are being administered to patients for enhanced safety of smart infusion systems. The nanoreplica molding method used to make the nanodome substrates is a low-cost, mass-manufacturing process which would allow the devices to be adopted in a clinical setting as disposable single-use sensors. We plan to further test this approach for the detection of additional IV drugs and metabolites within urine and actual blood samples. We also plan to investigate the potential for developing nanodome sensors fabricated upon thin plastic substrates that are highly flexible so that they may be attached to curved surfaces, and incorporated directly into the inner surface of cylindrical tubing. This sensor approach may be applied to the internal surface of many types of liquid containers (test tubes, flasks, graduated cylinders) for a wide range of applications including but not limited to medical detection, food processing, and environmental monitoring.

Acknowledgements

The authors thank the staff of the Micro and Nanotechnology Laboratory and the Center for Nanoscale Chemical-Electrical-Mechanical Manufacturing Systems (Nano-CEMMS) at the University of Illinois at Urbana-Champaign. This material is based upon work supported by the National Science Foundation under Award No. DMI 0328162 and ECCS 09-24062. Any opinions, findings, and conclusions or recommendations expressed in this material are those of the author(s) and do not necessarily reflect the views of the National Science Foundation.

Notes and references

- 1 D. P. Phillips, N. Christenfeld and L. M. Glynn, *Lancet*, 1998, **351**, 643–644.
- 2 S. K. Steingass, *Journal of Nursing Administration*, 2004, **34**, 10–10.
- 3 U.S. Food and Drug Administration: Information for Healthcare Professionals - Intravenous Promethazine and Severe Tissue Injury, Including Gangrene, www.fda.gov.
- 4 W. R. Premasiri, R. H. Clarke and M. E. Womble, *Lasers Surg. Med.*, 2001, **28**, 330–334.
- 5 A. Radoomska, R. Koncki, K. Pyrzynska and S. Glab, *Anal. Chim. Acta*, 2004, **523**, 193–200.
- 6 B. Premanode and C. Toumazou, *Sens. Actuators, B*, 2007, **120**, 732–735.
- 7 Y. Morishita, K. Nakane, T. Fukatsu, N. Nakashima, K. Tsuji, Y. Soya, K. Yoneda, S. Asano and Y. Kawamura, *Clinical Chemistry*, 1997, **43**, 1932–1936.

- 8 W. Sant, M. L. Pourciel, J. Launay, T. Do Conto, A. Martinez and P. Temple-Boyer, *Sens. Actuators, B*, 2003, **95**, 309–314.
- 9 A. Senillou, N. Jaffrezic-Renault, C. Martelet and S. Cosnier, *Talanta*, 1999, **50**, 219–226.
- 10 A. Sansubrin and M. Mascini, *Biosens. Bioelectron.*, 1994, **9**, 207–216.
- 11 A. S. Jdanova, S. Poyard, A. P. Soldatkin, N. Jaffrezic-Renault and C. Martelet, *Anal. Chim. Acta*, 1996, **321**, 35–40.
- 12 I. Basu, R. V. Subramanian, A. Mathew, A. M. Kayastha, A. Chadha and E. Bhattacharya, *Sens. Actuators, B*, 2005, **107**, 418–423.
- 13 J. V. de Melo, S. Cosnier, C. Mousty, C. Martelet and N. Jaffrezic-Renault, *Anal. Chem.*, 2002, **74**, 4037–4043.
- 14 R. A. Shaw, S. Kotowich, H. H. Mantsch and M. Leroux, *Clin. Biochem.*, 1996, **29**, 11–19.
- 15 M. Fleischmann, P. J. Hendra and A. J. McQuillan, *Chem. Phys. Lett.*, 1974, **26**, 163–166.
- 16 D. L. Jeanmaire and R. P. Van Duyne, *J. Electroanal. Chem.*, 1977, **84**, 1–20.
- 17 P. L. Stiles, J. A. Dieringer, N. C. Shah and R. R. Van Duyne, *Annu. Rev. Anal. Chem.*, 2008, **1**, 601–626.
- 18 C. J. Choi, Z. D. Xu, H. Y. Wu, G. L. Liu and B. T. Cunningham, *Nanotechnology*, 2010, **21**, 415301.
- 19 T. Brooks and C. W. Keevil, *Lett. Appl. Microbiol.*, 1997, **24**, 203–206.
- 20 A. W. Martinez, S. T. Phillips, M. J. Butte and G. M. Whitesides, *Angew. Chem., Int. Ed.*, 2007, **46**, 1318–1320.
- 21 K. R. Ackermann, T. Henkel and J. Popp, *ChemPhysChem*, 2007, **8**, 2665–2670.
- 22 D. Lin, S. Y. Feng, J. J. Pan, Y. P. Chen, J. Q. Lin, G. N. Chen, S. S. Xie, H. S. Zeng and R. Chen, *Opt. Express*, 2011, **19**, 13565–13577.
- 23 D. M. Shin, X. Wang, X. M. Qian, J. J. Beitler, Z. G. Chen, F. R. Khuri, M. M. Lewis, H. J. C. Shin and S. M. Nie, *Cancer Res.*, 2011, **71**, 1526–1532.
- 24 M. Casella, A. Lucotti, M. Tommasini, M. Bedoni, E. Forvi, F. Gramatica and G. Zerbi, *Spectrochim. Acta, Part A*, 2011, **79**, 915–919.
- 25 A. J. Haes, C. L. Haynes, A. D. McFarland, G. C. Schatz, R. R. Van Duyne and S. L. Zou, *MRS Bull.*, 2005, **30**, 368–375.
- 26 R. P. Van Duyne, J. P. Camden, J. A. Dieringer and J. Zhao, *Acc. Chem. Res.*, 2008, **41**, 1653–1661.
- 27 Z. D. Xu, M. R. Gartia, C. J. Choi, J. Jiang, Y. Chen, B. T. Cunningham and G. L. Liu, *J. Raman Spectrosc.*, 2011, **42**, 1939–1944.
- 28 K. B. Crozier, W. Q. Zhu, M. G. Banaee, D. X. Wang and Y. Z. Chu, *Small*, 2011, **7**, 1761–1766.
- 29 L. Dal Negro, A. Gopinath, S. V. Boriskina and B. M. Reinhard, *Opt. Express*, 2009, **17**, 3741–3753.
- 30 A. Gopinath, S. V. Boriskina, W. R. Premasiri, L. Ziegler, B. M. Reinhard and L. Dal Negro, *Nano Lett.*, 2009, **9**, 3922–3929.
- 31 N. B. Colthup, L. H. Daly and S. E. Wiberley, *Introduction to infrared and Raman spectroscopy*, Academic Press, 1990.
- 32 P. Vandenabeele, M. de Veij, T. De Beer, J. P. Remonc and L. Moens, *J. Raman Spectrosc.*, 2009, **40**, 297–307.
- 33 P. Vandenabeele, J. De Gelder, K. De Gussem and L. Moens, *J. Raman Spectrosc.*, 2007, **38**, 1133–1147.